Rapid-Charging Navigation of Electric Vehicles Based on Real-Time Power Systems and Traffic Data

Article *in* IEEE Transactions on Smart Grid · July 2014

DOI: 10.1109/TSG.2014.2309961

5 authors, including:

Qinglai Guo
Tsinghua University
120 PUBLICATIONS **485** CITATIONS
SEE PROFILE

Hongbin Sun
Tsinghua University
281 PUBLICATIONS **1,955** CITATIONS
SEE PROFILE

Zhengshuo Li
Tsinghua-Berkeley Shenzhen Institute
29 PUBLICATIONS **130** CITATIONS
SEE PROFILE

B.H. Zhang
Xi'an Jiaotong University
320 PUBLICATIONS **1,710** CITATIONS
SEE PROFILE

Rapid-Charging Navigation of Electric Vehicles Based on Real-Time Power Systems and Traffic Data

Qinglai Guo, *Senior Member, IEEE*, Shujun Xin, *Student Member, IEEE*, Hongbin Sun, *Senior Member, IEEE*, Zhengshuo Li, *Student Member, IEEE*, and Boming Zhang, *Fellow, IEEE*

***Abstract*—Electric vehicles (EVs) have attracted growing attention in recent years. However, daily charging of EVs, in particular rapid charging, may impact power systems, especially during peak hours, and the effects may occur in different places as traffic conditions change. To address these issues, we describe an integrated rapid-charging navigation strategy that considers both the traffic conditions and the status of the power grid. The system is based on an intelligent transport system (ITS), and contains four modules: a power system control center (PSCC), an ITS center, charging stations, and EV terminals. The PSCC calculates the available charging capacity and station charging capacity based on power grid data and transmits the results to the charging stations. The charging stations determine their charging plans and estimate the available charging power for future EVs (CPFE), and transmit these data to the ITS center. After receiving CPFE data and traffic data from the ITS center, the EV terminal estimates the total time for charging (TTC) for different stations, which includes the driving time, waiting time, and charging time. The driver can view these results and choose to be navigated to the charging station corresponding to the minimum TTC. The modular design of the navigation system reduces data transmission, which protects the drivers' privacy since they can choose which charging station to use and are not required to send any data to the ITS system. Simulation results demonstrate the feasibility of the proposed method for different working conditions for power system and traffic conditions.**

***Index Terms*—Charge, distribution network, electric vehicle (EV), traffic control.**

Nomenclature

ACC	Available charging capacity.
CPFE	Charging power for future EVs.
SCC	Station charging capacity.
TTC	Total time for charging.
T_0	Time interval for load prediction.
$SCC_{i,k}^{A,B,C}/P_{i,k}^{A,B,C}/Q_{i,k}^{A,B,C}/V_{i,k}^{A,B,C}/\delta_{i,k}^{A,B,C}$	Three-phase SCC/power/reactive power/voltage/phase angle of node i between $[kT_0,(k+1)T_0)$.
$\eta_i/\overline{SCC_i}$	Power factor/higher limit of the SCC at charging station i.
$\underline{P_i}/\overline{P_i}$	Lower/upper power limit of the charging poles at charging station i.
$\underline{V_i^{A,B,C}}/\overline{V_i^{A,B,C}}$	Lower limit/higher limit of voltage of node i.
$\overline{I_{ij}^{A,B,C}}$	Three-phase current constraints of the branch ij.
$P_{\boldsymbol{i,t}}^{\mathrm{new}}$	CPFE for during $\mathcal{T}_{i,t}$.
$SOC_t/D_{i,t}$	EV state of charge/driving distance to charging station i at time t.
$E^{\mathrm{finish}}/E_{\mathrm{drive}}$	EV energy storage after charging/energy consumption rate per km.
$E_{ca}/E_{ca}^{\min}$	Energy capacity/minimum energy storage of the EV battery.
$\mathcal{T}_{i,t}$	Set of all time windows for the charging plan.
$T_{i,t}^{\mathrm{drive}}/T_{i,t}^{\mathrm{wait}}/T_{i,t}^{\mathrm{charge}}/T_i^{sw}$	Driving/waiting/charging/battery switching time.

Manuscript received September 16, 2013; revised January 05, 2014; accepted February 20, 2014. Date of publication April 25, 2014; date of current version June 18, 2014. This work was supported by the National Key Basic Research Program of China (973 Program) (2013CB228202), the National Science Fund for Distinguished Young Scholars (51025725), and the Tsinghua University Initiative Scientific Research Program. Paper no. TSG-00735-2013.

The authors are with the Department of Electrical Engineering, Tsinghua University, Beijing 100084, China (e-mail: shb@mail.tsinghua.edu.cn).

Color versions of one or more of the figures in this paper are available online at http://ieeexplore.ieee.org.

Digital Object Identifier 10.1109/TSG.2014.2309961

I. Introduction

With growing concern about the sustainability of energy resources and climate change, there has been much recent interest in electric vehicles (EVs) [1], [2]. EVs are zero-emission during driving and can be more energy-efficient than conventional vehicles with combustion engines. Besides, through proper regulation, EV charging loads could be utilized to help integrate renewable but intermittent energy sources for further carbon emission reduction as well [3]–[5]. Though the EV have not been widely used now, it is expected to become an integral part of the traffic. In the USA, the Obama administration has embraced a goal of having one million electric-powered vehicles by 2015 [6]. Recently, a number of car manufactures, including Nissan and Toyota, have already developed commercially available electric vehicles [7]–[9]. The necessary infrastructure, including the charging stations and charging poles, is currently being expanded in a number of countries across the world.

However, as the number of EVs grows, the heavy and unpredictable loads due to charging may cause problems for the power system, such as thermal overloads and

under-voltages [10]–[12]. In order to mitigate these effects, studies have been carried out focusing on optimized charging methods, including controlling the charging duration and rate [13]–[16], as well as using dynamic pricing to manage the time distribution of the load [17]–[21]. In most of these studies, the goals have been to shift the load or to ensure the reliability of large-scale power systems. By assuming that the charging power can be fully adjusted, and the charging rate can be slowed down, these optimization methods have mainly been applied to residential charging, especially during the night when large numbers of EVs are plugged in. The charging facility can be viewed as an ordinary residential electric device and it can be connected directly to low voltage distribution system.

Besides slow charging method, rapid charging method should also be considered. Slow charging method takes 6–8 hours, mostly for long-term parked EVs, while the rapid charging method supplies higher power, which can reach 50–100 kW [22], so that charging occurs over 15 minutes to 2 hours. However, it requires specific charging facilities and mostly takes place in commercial charging stations [23]. Because of the shorter charging time, some EV drivers may choose this method to continue their driving soon. It is especially applicable to those drivers who consume large amounts of energy and have a long-distance trip, such as taxi and shuttle drivers.

Obviously, different from wide-spreading and low-power residential charging, rapid charging loads in charging stations are much more concentrated and heavy. Because of its high power level, rapid charging stations should be connected to medium voltage distribution system in three-phase rather than to low voltage distribution system in single-phase [22], [24]. In China, most rapid charging stations are connected to 10-kV feeder in three-phase [25].

Therefore, analyzing impact of rapid charging load should also take power system structure into consideration rather than a simple load curve [23]–[27]. Besides, as rapid charging station operation is affected by traffic a lot, both planning [28], [29] and load analyzing [30]–[32] of rapid charging station should consider traffic factor. In [32], a mathematical model of the EV charging demand for a rapid-charging station was reported and used to analyze the expected charging loads at different exits of a highway. This model used fluid dynamics to describe the arrival rate of EVs to aid the forecasting of demand and construction planning of charging stations.

When operating a rapid-charging station, it is necessary not only to analyze the additional demand due to EV charging, but also to develop a strategy to mitigate the impact on the grid and maximize the available rapid-charging power during operation. In contrast to the adjustable slow-charging method, rapid charging offers high power immediately following the start of charging, so that the controlling strategies for slow-charging method cannot employ temporal optimization. In this case, with considering EV drivers' subjectivities, spatial optimization may be a more valuable approach. There are two aspects to the optimization of EV charging considered here. First, the driver should reach the charging station as soon as possible; second, the load should have minimal impact on the operation of the power grid.

Now, GPS-based navigation systems are installed in many vehicles, which are employed to navigate the vehicle to a certain destination and can be utilized for EV charging navigation. Some applications are even able to account for real-time traffic information to select routes that avoid traffic congestion, such as Baidu Map [33], which also has a phone version, and it offers application programming interface (API) for software developing [34]. However, such navigation cannot consider the power system information or constraints. Sometimes, distribution system may be partially overloaded because of unexpectable reasons, such as residential air conditioning load in an extremely hot day, or sudden change of distributed generation's (DG's) power output. Under these scenarios, if too many EVs are guided to a charging station and the feeder this charging station connected to has already been overloaded, this local overload may become more serious. Besides, compared with other power loads, spatial distribution of EV rapid charging load is easier and more applicable to adjust to help alleviate local overload of the power system, thus ensure safety of the power system. Therefore, it could be beneficial to consider the spatial distribution of the load due to EV charging when providing route information to drivers.

A navigation strategy considering power grid operation that revises the traffic distance to an electrical distance has been reported previously [35], where the basic architecture of the charging and navigation system was introduced. However, it is difficult to transform the power system information into a distance term, and the system might not be exploited by EV drivers, who may choose to disregard the proposed routes because the electrical distance makes little sense to them. Here, we report a follow-up study, where we aim to build a more integrated navigation system and put forward a more practical and efficient navigation strategy.

There are two major challenges that must be addressed to implement such an integrated navigation system. The first is finding a suitable method of transforming the demand on the operation of the power grid into the navigation of EVs. In this paper, traffic and power grid information are unified into a "*time*" term, and the drivers are expected to choose the option that is the least time consuming, where this time includes the driving time, waiting time, and charging time. The second challenge is reducing the information exchange as well as protecting the drivers' privacy during navigation. To solve these problems, an integrated architecture was designed in a modular fashion. Each module performs calculations locally, reducing the data exchange required between modules compared with a centralized calculation method. The EV terminal can complete the calculations and determine the best route based on broadcast data about the status of the power grid and the traffic system. No data about the EV will be sent to the server, which ensures the privacy of the driver.

The remainder of this paper is organized as follows. Section II introduces the intelligent transport system (ITS) as well as the architecture of the integrated charging guide system. Section III describes the functions and strategies of each system module as well as the data transmission between modules, and presents a minimum total time for charging (TTC) strategy, then discusses how this charging navigation method helps reduce information transmission and protect privacy. Section IV presents a simulation example to assess the performance of the navigation strategy. Section V concludes with a summary of the study findings.

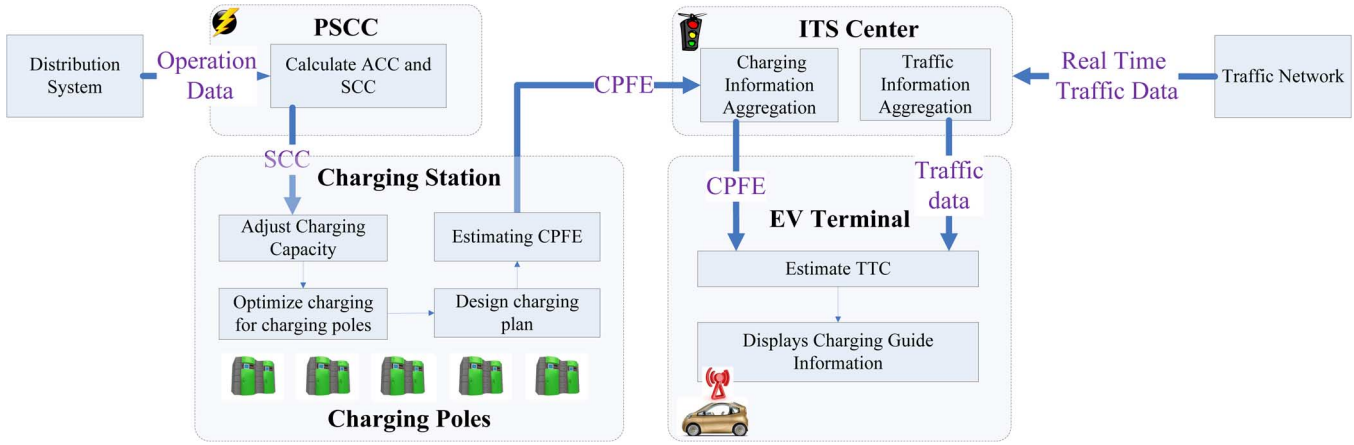

Fig. 1. Working process of the integrated charging controlling system.

II. Architecture

To effectively apply a navigation strategy that considers the location of charging stations, a comprehensive system that combines the power grid data and traffic data is required. The power grid data may be obtained from a network control center, and the traffic data may be obtained from an intelligent transport system (ITS).

A. Brief Introduction of ITS

An ITS is a transport management system where the goal is to reduce traffic congestion by optimizing the routing of vehicles. It integrates advanced information, data communication, electronic sensor, and electronic control technologies [36]–[40]. Now many countries are actively developing this technology, including the USA and China [41], [42].

There are many applications of ITS technologies, of which the most widely-used one is vehicle navigation system. In order to implement location and navigation, vehicle navigation system includes geographic information systems (GIS), global positioning system (GPS), image monitoring, and wireless communication technology [43], [44]. Besides, vehicle navigation system is able to obtain real-time traffic data with other assistive tools, such as Traffic Message Channel (TMC) [45] and Vehicle Information and Communication System (VICS) [46]. These tools allow delivery of dynamic traffic information to vehicle terminals through conventional FM radio broadcasts without interrupting normal broadcast services [47]. The real-time traffic data could be utilized to improve navigation by avoid traffic congestion [48].

B. Architecture Design

A driver of an EV first considers whether the state of charge (SOC) of the EV is sufficient for the desired journey. If not, they will consider how to recharge the EV as quickly as possible. An integrated charging navigation system should be able to respond to the charging demand of the EV and navigate the EV to a charging station afterwards, minimizing the overall journey time.

To ensure reliability of the power system, if a feeder has a high load level, the available power at a charging station connected to this feeder should be limited. Therefore, properly distributing charging load to different rapid-charging stations should be required and beneficial. To perform these two functions, the proposed system contains four modules: a power system control center (PSCC), an ITS center, charging stations, and EV terminals. The system structure is shown in Fig. 1.

The PSCC evaluates the stability of the power system and determines SCC of each charging station. The charging station further optimizes the charging power of each pole based on SCC and estimates charging power for future EVs (CPFE). The ITS center receives data from both charging stations and traffic network, then releases them to the public. The EV terminal calculates TTC for each charging station after receiving information released by the ITS center, then displays the result to the driver and shows the journey data after the driver determines where to charge.

During operation, information about the grid, charging stations, traffic, and EV is used, and most information is analyzed where it is gathered, so data transmission is reduced as much as possible. In this system, the PSCC and ITS centers do not require data about the EV to make decisions, and EV drivers decide where to charge by comparing the different times for different options. EV drivers are not required to upload information such as the SOC or spatial location.

III. Methods

A. PSCC Strategy

Charging stations are distributed at different feeders of the distribution system. The maximum charging power of each charging station should be limited for the safety of the power system. Define the maximum charging power of each station as the station charging capacity (SCC).

The maximum permissible charging load of all rapid-charging stations, defined as the available charging capacity (ACC), can be calculated through summing SCCs. ACC could represent charging capacity of the whole system.

System controllers hope to maximize ACC without harming the safety of power system. Therefore, PSCC needs to optimize ACC for the system and SCC for each charging station.

As mentioned before, because of high power level, rapid charging station is connected to medium voltage distribution system in three-phase. With AC/DC converter, charging station could adjust charging load on each phase. Therefore, the optimization of ACC and SCC should consider three-phase distribution system model. The SCC as well as the ACC during

$[kT_0,(k+1)T_0)$, can be calculated by assuming the slack bus of the system is the root node, whose process is shown as follows:

$$
\begin{aligned}
&\max_{SCC_k} \sum_{\mathrm{i}\in\lambda} SCC_{i,k}\\
&s.t.\\
&SCC_{i,k} = SCC_{i,k}^{A} + SCC_{i,k}^{B} + SCC_{i,k}^{C} \quad \mathrm{i}\in\lambda\\
&P_{i,k}^{A,B,C} - V_{i,k}^{A,B,C} * \sum_{j\in i} V_{j,k}^{A,B,C} *\\
&\quad \left(G_{ij}^{A,B,C}\cos\delta_{ij,k}^{A,B,C} + B_{ij}^{A,B,C}\sin\delta_{ij,k}^{A,B,C}\right) = 0 \quad \mathrm{i}\notin\lambda\\
&Q_{i,k}^{A,B,C} + V_{i,k}^{A,B,C} * \sum_{j\in i} V_{j,k}^{A,B,C} *\\
&\quad \left(B_{ij}^{A,B,C}\cos\delta_{ij,k}^{A,B,C} - G_{ij}^{A,B,C}\sin\delta_{ij,k}^{A,B,C}\right) = 0 \quad \mathrm{i}\notin\lambda\\
&SCC_{i,k}^{A,B,C} + P_{i,k}^{A,B,C} - V_{i,k}^{A,B,C} * \sum_{j\in i} V_{j,k}^{A,B,C} *\\
&\quad \left(G_{ij}^{A,B,C}\cos\delta_{ij,k}^{A,B,C} + B_{ij}^{A,B,C}\sin\delta_{ij,k}^{A,B,C}\right) = 0 \quad \mathrm{i}\in\lambda\\
&\frac{\sqrt{1-\eta_i^2}}{\eta_i} SCC_{i,k}^{A,B,C} + Q_{i,k}^{A,B,C} + V_{i,k}^{A,B,C} * \sum_{j\in i} V_{j,k}^{A,B,C} *\\
&\quad \left(B_{ij}^{A,B,C}\cos\delta_{ij,k}^{A,B,C} - G_{ij}^{A,B,C}\sin\delta_{ij,k}^{A,B,C}\right) = 0 \quad \mathrm{i}\in\lambda\\
&\underline{V_i^{A,B,C}} \le V_{i,k}^{A,B,C} \le \overline{V_i^{A,B,C}} \quad \forall \mathrm{i} = 1,2,\ldots,N\\
&\left|\left(g_{ij}^{A,B,C} + j\times b_{ij}^{A,B,C}\right)\left(V_{i,k}^{A,B,C} - V_{j,k}^{A,B,C}\right)\right|\\
&\quad < \overline{I_{ij}^{A,B,C}} \quad \forall \mathrm{i} = 1,2,\ldots,N, j\in i\\
&0 \le SCC_{i,k} \le \overline{SCC_i} \quad \forall \mathrm{i}\in\lambda\\
&P_{i,k}^{A,B,C} = \left[P_{i,k}^{A}\ P_{i,k}^{B}\ P_{i,k}^{C}\right]^T \quad Q_{i,k}^{A,B,C} = \left[Q_{i,k}^{A}\ Q_{i,k}^{B}\ Q_{i,k}^{C}\right]^T\\
&\quad V_{i,k}^{A,B,C} = \left[V_{i,k}^{A}\ V_{i,k}^{B}\ V_{i,k}^{C}\right]^T \quad \forall \mathrm{i} = 1,2,\ldots,N\\
&\delta_{ij,k}^{A,B,C} = \left[\delta_{i,k}^{A} - \delta_{j,k}^{A}\ \delta_{i,k}^{B} - \delta_{j,k}^{B}\ \delta_{i,k}^{C} - \delta_{j,k}^{C}\right]^T\\
&\qquad \forall \mathrm{i} = 1,2,\ldots,N, j\in i\\
&V_{0,k}^{A,B,C} = [V_0\ V_0\ V_0]^T \quad \delta_{0,k}^{A,B,C} = [0\ 0\ 0]^T\\
&SCC_{i,k}^{A,B,C} = \left[SCC_{i,k}^{A}\ SCC_{i,k}^{B}\ SCC_{i,k}^{C}\right]^T \quad \forall \mathrm{i}\in\lambda\\
&\underline{V_i^{A,B,C}} = \left[\underline{V_i^{A}}\ \underline{V_i^{B}}\ \underline{V_i^{C}}\right]^T\\
&\quad \overline{V_i^{A,B,C}} = \left[\overline{V_i^{A}}\ \overline{V_i^{B}}\ \overline{V_i^{C}}\right]^T \quad \forall \mathrm{i} = 1,2,\ldots,N\\
&\overline{I_{ij}^{A,B,C}} = \left[\overline{I_{ij}^{A}}\ \overline{I_{ij}^{B}}\ \overline{I_{ij}^{C}}\right]^T \quad \forall \mathrm{i} = 1,2,\ldots,N, j\in i
\end{aligned}
\tag{1}
$$

where the operator $*$ represents Hardmard product of two matrices.

In formula (1), $P_{i,k}^{A,B,C}$ and $Q_{i,k}^{A,B,C}$ represent three-phase active power and reactive power of node i during $[kT_0,(k+1)T_0)$ obtained from conventional load demand prediction, where T_0 is the time interval for load prediction. G and B are real and imaginary parts of the three-phase nodal admittance matrix. g and b are real and imaginary parts of the three-phase branch admittance matrix. λ represents the set of nodes consisting of rapid-charging stations.

For a certain charging station i, its SCC during $[kT_0,(k+1)T_0)$ is represented by $SCC_{i,k}$, which equals to the sum of SCC on three phases $SCC_{i,k}^{A}$, $SCC_{i,k}^{B}$ and $SCC_{i,k}^{C}$. If the station has l_i identical charging poles, the total charging power of which is in the range $[\underline{P_i},\overline{P_i}]$, then $\overline{SCC_i} = l_i\overline{P_i}$.

Following these calculations, the PSCC will distribute the SCC to each station. The data structure is shown as follows:

$$
\begin{Bmatrix}
i & //\text{location of the charging station}\\
[kT_0,(k+1)T_0) & //\text{SCC time window}\\
\mathrm{SCC}_{i,k} & //\text{SCC value}\\
SCC_{i,k}^{A}, SCC_{i,k}^{B}, SCC_{i,k}^{C} & //\text{SCC limit on each phase}
\end{Bmatrix}.
\tag{2}
$$

B. Charging Station Strategy

After receiving the SCC reference value from the PSCC, the charging station must optimize the available power for each charging pole, design a charging plan, and predict the charging demand in the future. The charging station then sends its operating data to the ITS center, which is then released to the public.

1) Power Optimization for Charging Poles: The charging station must optimize the available power at each charging pole after receiving the SCC data. During this process, four factors should be considered.

a) To ensure fairness, the SCC should be equally distributed to each operating charging machine.
b) To maximize the number of EVs that can be charged, the number of working charging poles should be maximized.
c) To ensure reliability, the charging power of each charging pole at charging station i should be in the range $[\underline{P_i},\overline{P_i}]$.
d) Charging of the EVs should not be interrupted or terminated early.

When optimizing charging power, b is the optimization objective, and a, c, and d are the constraints. The optimization results will remain constant unless an EV finishes charging or the SCC changes. The optimization is as follows:

$$
\begin{aligned}
&\max_{\inf(\mathcal{T})=t} n_{i,\mathcal{T}}\\
&\text{s.t.}\quad 1 \le n_{i,\mathcal{T}} \le l_i && (3.1)\\
&\qquad n_{i,\mathcal{T}} \le m_{i,t} && (3.2)\\
&\qquad \frac{SCC_{i,k}}{n_{i,\mathcal{T}}} \ge \underline{P_i}\,\mathcal{T}\in[kT_0,(k+1)T_0) && (3.3)\\
&\qquad \frac{SCC_{i,k+1}}{n_{i,\mathcal{T}}} \ge \underline{P_i} \text{ if } \sup(\mathcal{T}) = (k+1)T_0 && (3.4)
\end{aligned}
\tag{3}
$$

where $\mathcal{T}$ is the time window of the optimization, which begins from the current time and ends when an EV finishes charging or the SCC changes; $n_{i,\mathcal{T}}$ is the number of EVs currently charging at station i; and $m_{i,\mathcal{T}}$ is the total number of EVs.

The charging power at each charging pole can be obtained from

$$
P_{i,\mathcal{T}} = \min\left(\frac{SCC_{i,k}}{n_{i,\mathcal{T}}}, \overline{P_i}\right) \tag{4}
$$

During the optimization, the upper limit of $\mathcal{T}$ is unknown, so constraint (3.4) cannot be considered at first. It will instead be used to verify and revise the results.

Without considering constraint (3.2), the optimization is the theoretical maximum number of charging EVs, recorded as $n'_{i,\mathcal{T}}$. If $n'_{i,\mathcal{T}}$ is greater than $n_{i,\mathcal{T}}$, no EVs are waiting to charge

so that if another EV reaches charging station i at that instant in time, it can be charged immediately.

2) Charging Plan Designing: If the SCCs in the following time windows are already known, the charging plan of all EVs in the station can be obtained through the following process.

a) Optimize the charging rates for the current time (see Section III-B-1).
b) Recalculate the SOC of all EVs at charging station i at the end of $\mathcal{T}$.
c) Set the current time to $t = \sup(\mathcal{T})$. Go to step a) and continue optimization

Through this process, charging plans for all EVs at the station can be calculated. Assuming that the time windows for each optimization are $\mathcal{T}_{i,1} \ldots \mathcal{T}_{i,w}$, $\mathcal{T}_{i,t} = \{\mathcal{T}_{i,1} \ldots \mathcal{T}_{i,w}\}(\inf(\mathcal{T}_{i,1}) = t)$ can be regarded as the total time for the charging plan. In the absence of new EVs arriving at the charging station, the charging plan does not change.

3) Estimating the Charging Power for Future EVs (CPFE): Let the current and theoretical maximum number of charging EVs be $n_{i,j}$ and $n'_{i,j}$, and let the charging power of each pole during $\mathcal{T}_{i,j}$ be $P_{i,j}$ $(j = 1 \ldots w)$. If an EV arrives at the charging station during $\mathcal{T}_{i,j}$, the immediate charging power should be

$$P_{i,j}^{\text{new}} = \begin{cases} 0, & \text{if } \exists l \geq j n'_{i,j} = n_{i,j} \\ \min\left(\frac{SCC_{i,k}}{n_{i,j}+1}, \overline{P_i}\right), & \text{else} \end{cases} \tag{5}$$

where k satisfies $\mathcal{T}_{i,j} \in [kT_0, (k+1)T_0)$.

The CPFE at station i can be represented by $\boldsymbol{P}_{\boldsymbol{i,t}}^{\text{new}} = \{P_{i,1}^{\text{new}}, \ldots, P_{i,w}^{\text{new}}\}$. It should be recalculated only when the charging plan changes.

4) Data Transmission to the ITS Center: For each charging station, only $\mathcal{T}_{i,t}$ and the CPFE data must be uploaded to the ITS center. These must be recalculated and uploaded when the charging plan changes. The data structure is as follows:

$$\left\{ \begin{array}{l} \text{i} \qquad \text{//location of the charging station} \\ \mathcal{T}_{i,t} = \{\mathcal{T}_{i,1} \ldots \mathcal{T}_{i,w}\} \\ \boldsymbol{P}_{\boldsymbol{i,t}}^{\text{new}} = \left\{P_{i,1}^{\text{new}}, \ldots, P_{i,w}^{\text{new}}\right\} \end{array} \right\}. \tag{6}$$

C. ITS Center

The main task of the ITS center is to collect the CPFE from each charging station and transmit it to each EV. The ITS center also gathers real-time traffic data and transmit this to the EV terminals for navigation purposes. The center does not require any information from the EVs.

D. EV Terminal and Minimum TTC Strategy

The time to recharge EVs should be minimized, so the navigation should minimize the TTC, which starts at the current time and ends when the EV is fully charged. There are three steps for the driver to follow to recharge their EV: driving to a charging station; waiting for charging, if necessary; and recharging the EV.

The EV terminal is part of the ITS architecture, so it can receive real-time traffic data for route planning. The terminal may also receive charging station information from the ITS center, and may estimate the time until charging is complete using each charging station. Let the current time be t. The TTC for station i can be estimated as follows:

$$TTC_{i,t} = T_{i,t}^{\text{drive}} + T_{i,t}^{\text{wait}} + T_{i,t}^{\text{charge}} \tag{7}$$

where $T_{i,t}^{\text{drive}}$ is the driving time to station i, $T_{i,t}^{\text{wait}}$ is the waiting time at station i, and $T_{i,t}^{\text{charge}}$ is the charging time of station i.

1) Driving Time $T_{i,t}^{\text{drive}}$: $T_{i,t}^{\text{drive}}$ is the estimated minimum driving time from the current location to charging station i. With considering real-time SOC and remaining EV battery energy for driving, the calculation process of driving time $T_{i,t}^{\text{drive}}$ is presented below:

a) Calculate the EV's maximum driving distance with the remaining energy $D_t^{\max}$ through the formula below:

$$D_t^{\max} = \frac{E_{ca} SOC_t - E_{ca}^{\min}}{E_{\text{drive}}} \tag{8}$$

where E_{ca} represents energy capacity of the battery, $E_{ca}^{\min}$ represents the minimum energy storage of the battery, E_{drive} represents energy consumption per unit driving distance, and SOC_t represents EV's SOC at time t.

b) Search for all driving routes from current location to the charging station i and select those which are shorter than $D_t^{\max}$. If all driving routes are longer than $D_t^{\max}$, it means that the EV cannot reach the charging station i with the remaining battery energy. In this case, navigate the EV to this charging station is inapplicable, so there is no need to calculate TTC for this charging station. If there are some routes shorter than $D_t^{\max}$, go to the next step to calculate $T_{i,t}^{\text{drive}}$.
c) Estimate driving time corresponding to each route based on the real-time geographic and traffic information and choose the minimum one as $T_{i,t}^{\text{drive}}$. Set the distance of this route as $D_{i,t}$ and store path information of the route for future navigation.

Since the energy consumption rate, real-time SOC, battery capacity, and driving route are all known, the energy state when the EV reaches charging station i, E_i^{reach}, can be calculated as follows:

$$E_i^{\text{reach}} = E_{ca} SOC_t - E_{\text{drive}} D_{i,t}. \tag{9}$$

2) Waiting Time $T_{i,t}^{\text{wait}}$: $T_{i,t}^{\text{wait}}$ is the waiting time after the EV arrives at charging station i, which can be calculated from

$$T_{i,t}^{\text{wait}} = \max\left(0, \underline{\mathcal{T}_{i,j_0}} - t - T_{i,t}^{\text{drive}}\right) j_0 = \min_j (P_{i,j}^{\text{new}} > 0) \tag{10}$$

where $\underline{\mathcal{T}_{i,j_0}}$ is the starting time of time window $\mathcal{T}_{i,j_0}$.

If a given EV can be charged at rapid-charging station i immediately after arriving, it does not need to wait, and $T_{i,t}^{\text{wait}} = 0$. Otherwise, it must wait.

Only when the CPFE of the charging station is greater than 0 can a newly arriving EV be charged. The waiting time is $\underline{\mathcal{T}_{i,j_0}} - t - T_{i,t}^{\text{drive}}$.

3) Charging Time $T_{i,t}^{\text{charge}}$: Based on CPFE data received from the ITS center, the charging energy at a given time interval can be estimated from

$$E_{\text{i}}^{\text{charge}}(t_1,t_2)=\int_{T=t_1,}^{t_2} P_{i,j}^{\text{new}} T dT \quad T\in\mathcal{T}_{i,j} \tag{11}$$

where t_1 is the start time and t_2 is the end time for charging

The charging time $T_{i,t}^{\text{charge}}$ is the solution to the following equation:

$$E_{\text{i}}^{\text{charge}}\left(t_i^{\text{start}}, t_i^{\text{start}}+T_i^{\text{charge}}\right) = E^{\text{finish}} - E_{ca}SOC_t - E_{\text{drive}}D_{i,t} \tag{12}$$

in which E_{ca} represents energy capacity of the battery and t_i^{start} can be calculated through the formula as follows:

$$t_i^{\text{start}} = t + T_{i,t}^{\text{drive}} + T_{i,t}^{\text{wait}}. \tag{13}$$

After calculating TTCs for all reachable charging stations, the EV terminal will choose the charging station corresponding to the minimum TTC as destination and display navigation information to the EV driver.

E. Battery Switching Station

Besides directly charging, battery switching is another way to supply energy for EVs [49]. In China, battery switching facilities and stations are also expanded in many cities by State Grid Corporation of China [50]. Compared with normal residential charging method, battery switching takes less time and can only be finished by specialized exchanging terminals [49], [51]–[53], which is quite similar to rapid charging method. Based on these similarities, we regard the battery switching method as a special kind of charging, and bring it into our charging navigation strategy to enlarge its application range.

However, different from rapid charging station, the optimization inside the battery switching station could be simplified because the switching time is nearly the same for each battery. Besides, switched battery packets are coordinated charged and distributed by the State Grid Corporation [50], which indicates that all switched battery packets may be charged in a certain place other than in the battery switching stations. Therefore, battery switching station can be viewed as a simple battery transfer station without calculating its impact to the power grid.

The CPFE information for battery exchanging stations sent to the ITS center is defined as follows:

$$\left\{\begin{array}{ll} \text{i} & \text{//location of the battery exchaging station} \\ t_i^{sw} & \text{//the time after which a newly arriving EV} \\ & \text{can exchange its battery immediately} \\ T_i^{sw} & \text{//battery switching time} \end{array}\right\}. \tag{14}$$

In this case, the TTC for battery swapping station i can be calculated from

$$TTC_{i,t} = T_{i,t}^{\text{drive}} + T_{i,t}^{\text{wait}} + T_i^{sw}. \tag{15}$$

In (15), $T_{i,t}^{\text{drive}}$ is the driving time to station i, whose calculation process is shown in Section III-D1); T_i^{sw} is the battery switching time, which can be obtained from CPFE information (14); $T_{i,t}^{\text{wait}}$ is the waiting time at station i calculated through the following equation:

$$T_{i,t}^{\text{wait}} = \max\left(0, t_i^{ex} - t - T_{i,t}^{\text{drive}}\right). \tag{16}$$

F. System Overview and Privacy Protection

After estimating the TTC for each rapid charging/battery switching station, the driver can view these results from the terminal display and choose the best charging station and the corresponding route. As an EV driver may prefer to recharge their EV as soon as possible, they will tend to choose the station that corresponds to the minimum TTC rather than the minimum distance.

In this integrated charging navigation system, estimation and calculation are carried out locally, and only limited data need to be transmitted between modules.

Besides, each EV terminal is able to estimate TTC and plan driving route locally and independently using broadcast information of CPFE and traffic network. During calculation, the EV terminal transforms traffic and power grid information into time term for charging navigation without uploading any EV data to the upper center. Therefore, EV drivers' privacies are ensured.

In addition to traffic information, only CPFEs of rapid charging stations (battery switching stations) are transmitted [see data structures (2), (6) and (14)]. As the number of charging station is limited, data transmission is not challenging.

IV. Simulation and Case Study

In our previous work, we focused on a simulation method for the operation of EVs, where a hybrid simulation model was described [59]. As the movement of the EVs will affect the traffic and charging will affect the power system, this simulation should consider both traffic data and power data.

A. Simulation Model

1) Traffic System: Traffic data includes information on the transport network, including the length of the route and traffic speeds. However, compared with a real transport network, only a limited set of traffic data is required for the calculation, so simplification of the transport network is required first.

We considered a 15 × 15 km region of a city-center road network, containing four rapid-charging stations. The transport network and corresponding topological graph are shown in Fig. 2. Four rapid-charging stations (labeled CS1 to CS4) were located at transport nodes (T-nodes) 18, 31, 29, and 21.

Let the distance from T-node i to T-node j be L_{ij}, the original average traffic speed from T-node i to T-node j be s_{ij}^0, and the number of vehicles (including EVs and conventional vehicles) in the traffic flow from T-node i to T-node j be n_{ij}. The speed of the traffic flow is then

$$\overline{s_{ij}} = s_{ij}^0 \times f(n_{ij}, L_{ij}) \tag{17}$$

where $f(n_{ij}, S_{ij})$ is the correction function of the traffic speed according to the distribution of vehicles on the roads.

2) Distribution System: We considered the three-phase IEEE 33-node distribution system, as shown Fig. 3. The load curve at 96 points, which includes only conventional load demands, is

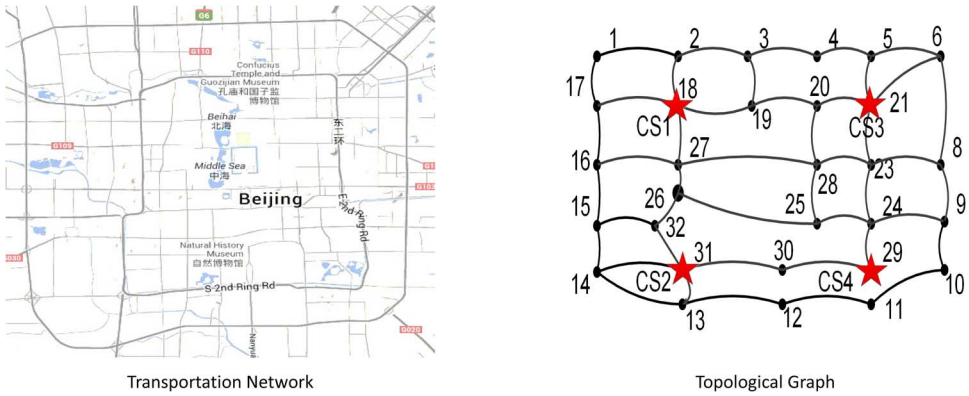

Fig. 2. Transportation network and its topological graph.

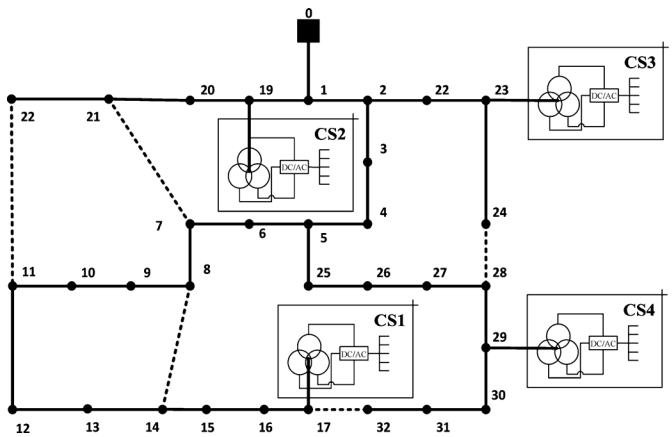

Fig. 3. Topological structure of IEEE-33 nodes standard distribution system.

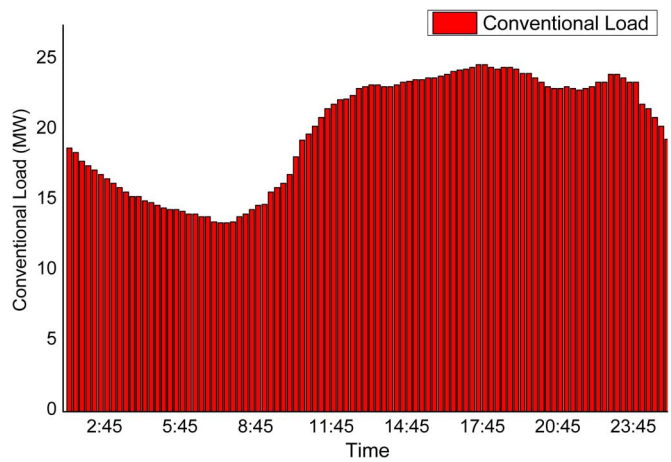

Fig. 4. 96 points' curve of other conventional loads of the system.

shown in Fig. 4. These data are from one day's operation data of a substation in Beijing, China.

Four rapid-charging stations are connected to the system in three-phase, respectively at nodes (D-nodes) 17, 19, 23, and 29, which are marked with CS1 to CS4 in Fig. 3. The parameters of the charging stations and EVs are listed in Section 0.

3) EV Model: Many studies have adopted specific travel datasets, such as the National Household Travel Survey (NHTS) [54], [55] and the National Travel Survey (NTS) [56], to sketch EV load models. In our simulation, EV model is built based on NHTS dataset to ensure that the simulation is consistent with the travel patterns of EV owners. NHTS includes the historical travel information of 150 147 households, including the number of daily trips, and the start and end times, distance, and purpose of each trip [57].

However, two points need to be noted in this simulation. First, only rapid charging demand and its distribution in the simulation area should be addressed. However, residential charging exists in our simulation. EVs will be plugged in to charge immediately after reaching destination through residential charging method. During simulation, only when an EV's energy storage cannot cover its current trip (from a certain origin to a certain destination) the EV needs to be charged in the rapid-charging station. Second, and most important, what we concerned about is rapid EV charging in the simulated area located in the city center, where traffic and power load vary a lot during the day, while residential areas are located in other places around the city, so EVs may not always run in the simulated area. For example, vehicles may enter or go through city center in the daytime and leave in the evening. Because of these two points, after generating background data structure, it is necessary to add spatial data to the origin dataset, whose process is presented as follows:

a) Set detailed origin and destination of each daily trip according to their types based on Beijing City Master Plan (2004–2020) [58].
b) Estimate detailed driving route of each vehicle trip through BaiduMap API [34]. If a driving route passes the simulated area, set Passing State of trip structure as 1, otherwise set it as 0.
c) If the Passing State of a driving route is 1, locate and record the places where the car starts at/enters and stops at/leaves the simulated area in the topological graph.
d) Estimate the time when the car starts at/enters the simulated area based on trip departure time and results from step b) and c).
e) Randomly set 3% vehicles as EVs.
f) Select vehicles which pass the simulated area during the day (at least one trip's Passing State is 1). These vehicles will be simulated in the case.
g) Add 2% shuttles and 5% taxis to our EV model.

After generating EV model, we can obtain an EV database for simulation with the data structure in Fig. 5:

4) Parameter Settings and Assumptions: Each rapid-charging station contained 12 charging machines, each with a capacity of 60 kW. The power factor was 0.96. The capacity of each EV was 60 kWh, and the energy consumption was

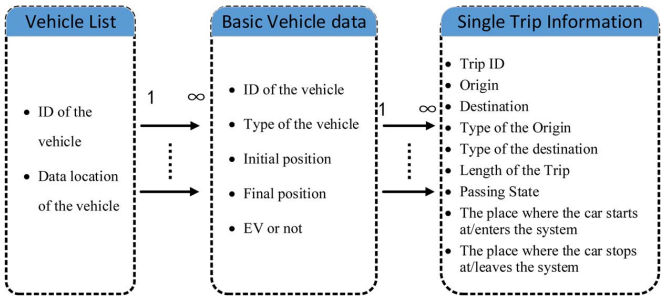

Fig. 5. Data structure of the EV database.

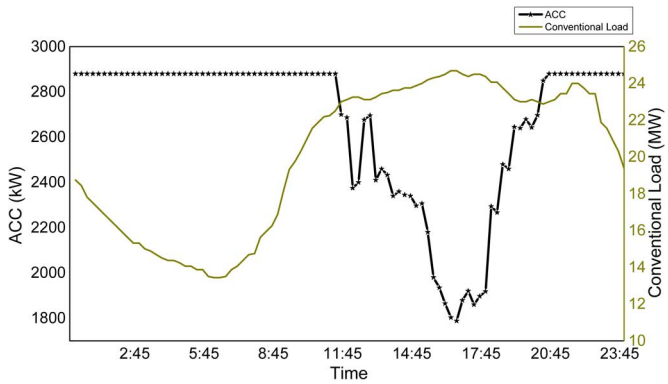

Fig. 6. ACC at different time.

assumed to be 0.18 kWh/km (these data apply to the Tesla Model S [7]). During simulation, the EV would be plugged in to charge at 5 kW after finishing a certain trip until the next trip took place, and only when an EV's energy storage was less than 40% and cannot afford its current trip the EV would choose to be charged in the rapid-charging station.

The initial average traffic speed at each road was set to 50 km/h. The correction function for the traffic speed was

$$f(n_{ij}, L_{ij}) = \begin{cases} 1 & \text{when } \frac{n_{ij}}{L_{ij}} \le 0.04 \\ 0.8 + 10\left(0.06 - \frac{n_{ij}}{L_{ij}}\right) & \text{when } 0.04 \le \frac{n_{ij}}{L_{ij}} \le 0.06 \\ 0.3 + 12.5\left(0.1 - \frac{n_{ij}}{L_{ij}}\right) & \text{when } 0.06 \le \frac{n_{ij}}{L_{ij}} \le 0.1 \\ 0.03\frac{L_{ij}}{n_{ij}} & \text{when } \frac{n_{ij}}{L_{ij}} \ge 0.1. \end{cases} \quad (18)$$

5) Traffic Simulation: The detailed simulation method is presented as follows:

a) Set the simulation parameters and navigation and charging strategy.
b) Utilize known load curves to calculate the ACC and SCC.
c) Generate detailed data about the EV based on NHTS and other known data.
d) Calculate the locations of each EV and the SOC. If an EV requires charging, calculate the optimum route according to the navigation and charging strategy.
e) Analyze the traffic flow on each road and the state of each charging station. If the SCC changes or a new EV arrives at a charging station, redesign the charging plan and recalculate the CPFE.
f) Record data at the current time and move the simulation forward one time-step.
g) If the time reaches the end time, stop the simulation or go back to step d) to continue.

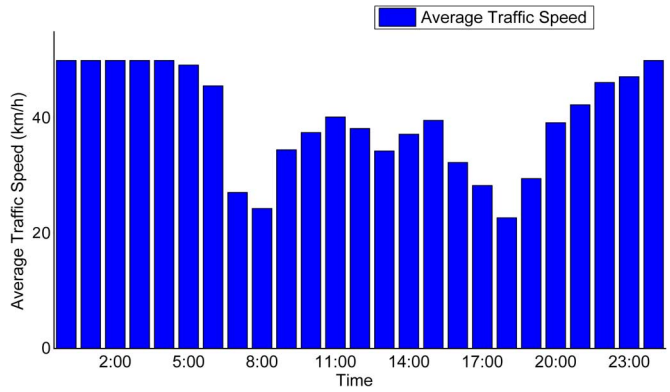

Fig. 7. Average traffic speed at different time.

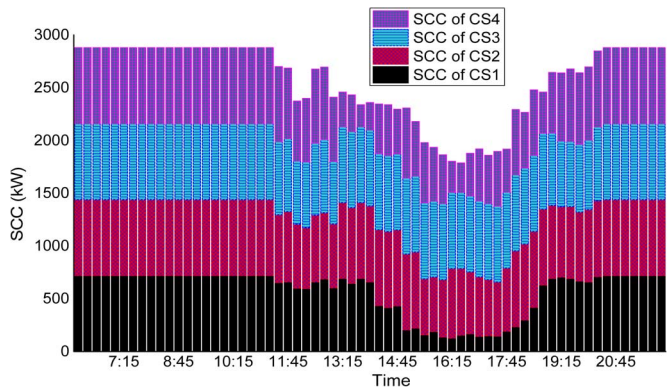

Fig. 8. ACC and SCCs at different time.

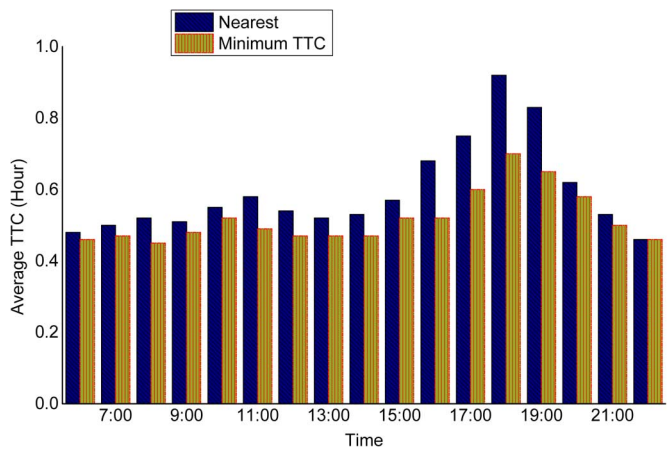

Fig. 9. Comparison of two charging guide strategies.

B. Simulation Results

The simulation considered 1 425 EVs and 36 724 conventional vehicles. The estimated TTC and simulated TTC were obtained when 286 EVs were charged between 6:00 to 21:00. The simulated data are shown in Figs. 6–10.

1) ACC and SCC: The ACC over one day is shown in Fig. 6. The time window was 15 minutes. The figure shows that the ACC changed during the daytime as other loads increased, and stayed at maximum value between 21:45 and 10:00 the next day. In other words, all charging stations could provide maximum power during that time, while the available power was limited between 10:00 and 22:00.

The average traffic speed is shown in Fig. 7. The traffic conditions changed significantly during the daytime hours between

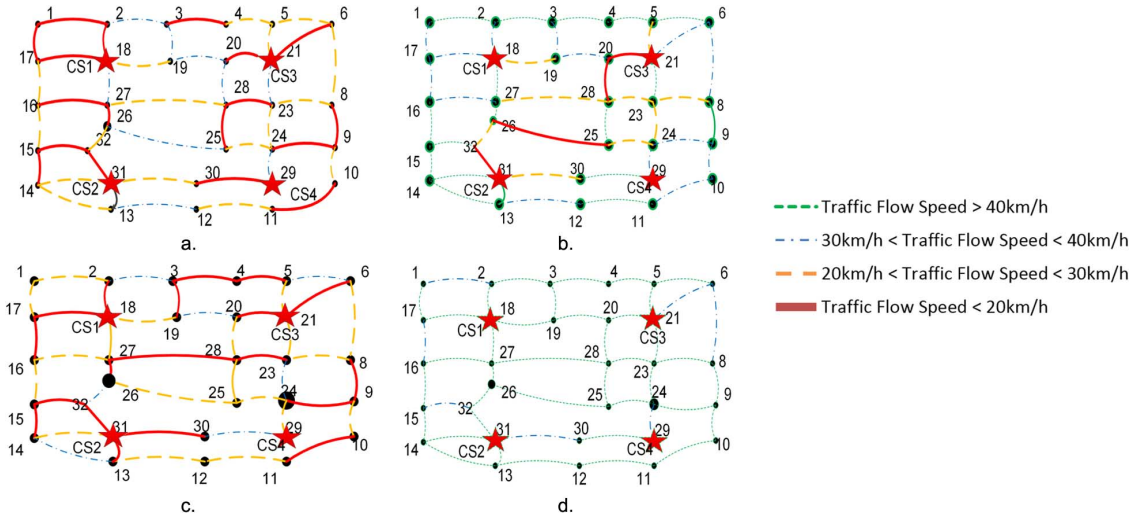

Fig. 10. Traffic condition at different time. (a) Traffic condition at 7:30. (b) Traffic condition at 12:30. (c) Traffic condition at 17:30. (d) Traffic condition at different time.

6:00 and 22:00. To better simulate and analyze the charging system and strategy, the simulation time was set between 6:00 and 22:00.

The SCC of each charging station between 6:00 and 22:00 was calculated as shown in Fig. 8. The SCC of each charging station decreased as the power load increased. However, the extent of the fluctuations of different charging stations differed. The SCC of CS1 and CS4 decreased more than that of CS2 and CS3 at peak hours. CS1 and CS4 were at the end of feeders, while CS2 and CS3 were closer to the root. To prevent transmission overload and voltage dips, the SCC of CS1 and CS4 should be reduced more during peak hours.

2) ACC and the Minimum TTC Strategy: In this section, the minimum TTC strategy is compared with another strategy, i.e., simply going to the nearest charging station, which is widely used in driving navigation

All the TTCs of the EVs were obtained from the simulation results, so the average TTC at different times could be calculated. Comparison of the average TTC of each charging guide strategy at different times is shown in Fig. 9.

Figs. 7–9 show that the TTC was affected by both the traffic conditions as well as ACC and SCCs. The traffic conditions at four typical times are shown in Fig. 10. From 6:00 to 10:00, the power load was light and traffic flow was heavy and all of the charging stations were able to provide full power. During this time, nearly all EVs could be recharged when they reached a charging station. However, the traffic flows were more congested at this time, and the minimum TTC strategy may help reduce the driving time for EVs because it assists drivers in choosing the best charging station and best routes. For example, in Fig. 10(a), driving from T-node 2 directly to T-node 18 was slower than driving from T-node 2, to T-node 3, and then to T-nodes 19 and 18, even though this latter route was more than twice as far.

Between 10:00 and 16:00, the power load on the grid increased, and the traffic flow decreased. As shown in Fig. 8, during this time, the SCCs of CS1 and CS4 decreased considerably, while those of the two other charging stations remained almost constant. Therefore, the difference in the average TTC was mainly caused by differences in the waiting time. The strategy of

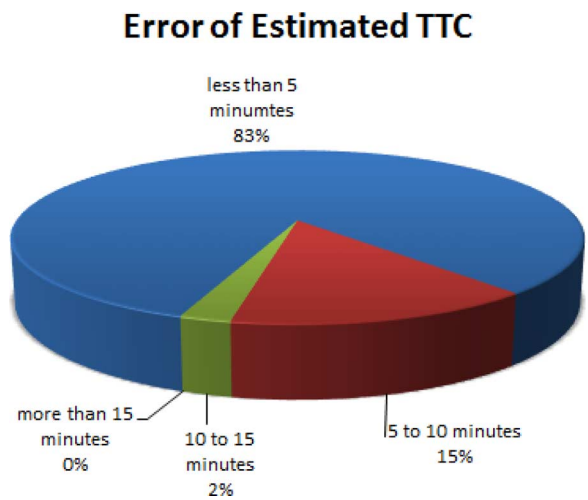

Fig. 11. Error condition of estimated TTCs.

going to the nearest charging station led to an excessive number of EVs waiting at CS1 and CS4, with some EVs waiting for over an hour before charging. In this case, CS2 and CS3 did not operate at full charging power. As traffic conditions improved [see Fig. 10(b)], driving to CS2 or CS3 required less time than waiting at CS1 or CS4. Because the minimum TTC strategy considers the SCCs of different charging stations and traffic data, it can be effective in reducing the TTC.

From 16:00 to 20:00, the power load was heavy and the traffic was slow. During this time, the SCC of CS1 and CS4 was significantly less than that of CS2 and CS3. The TTCs of both strategies were significantly longer than during other periods. However, Fig. 9 shows that the minimum TTC strategy reduced the average TTC by approximately 25% because it helps reduce both driving time and waiting time. After 20:00, the power load decreased and the traffic became faster. During this time, nearly all EVs could be charged quickly with both strategies because all stations were able to provide sufficient power and the number of EVs requiring power was small.

3) Accuracy of Estimated TTC: The difference between the estimated and simulated TTCs was calculated to determine the

error in the estimated values. This is shown in Fig. 11. Most of the errors were less than 10 minutes, and all of the errors were less than 15 minutes.

V. Conclusion

This paper presents a smart management method for rapid charging with consideration of spatial load distribution, which is an essential supplement for current residential charging controlling method through adjusting time and duration.

During charging navigation, both traffic data and power system data are considered and they are unified into time term by EV terminal for destination choosing. With considering its actual performance, the presented charging navigation system is built on module design. Each module transforms vast complex original data into simplified results and transmits them, which reduces data transmission of the system as well as calculation of upper control center. Furthermore, with this design, the information released by ITS center is easy to process by EV terminal. Therefore, the EV terminal could calculate TTC of each reachable charging station with the broadcast information.

Besides, the presented rapid charging navigation method also considers the demands as well as privacy of EV drivers. First of all, the index for charging navigation is minimum TTC, which meets drivers' needs especially during daytime. Besides, the EV terminal is able to estimate TTC locally using broadcast information without uploading any EV data to the upper center, so EV drivers' privacies are ensured.

In summary, the presented charging navigation method could satisfy drivers' demands with ensuring the security of the power grid, in which both electric and traffic factors are considered. This method is feasible through existing ITS techniques. Further researches will be focused on application of the presented method.

References

[1] S. G. Wirasingha and A. Emadi, "Pihef: Plug-in hybrid electric factor," *IEEE Trans. Veh. Technol.*, vol. 60, no. 3, pp. 1279–1284, Mar. 2011.

[2] EPRI, NRDC, "Environmental assessment of plug-in hybrid electric vehicles," Volume 1: Nationwide Greenhouse Gas Emissions Jul. 2007.

[3] H. Lund and W. Kempton, "Integration of renewable energy into the transport and electricity sectors through V2G," *Energy Policy*, vol. 36, pp. 3578–3587, 2008.

[4] S. Ramteen and P. Denholm, "Emissions impacts and benefits of plug-in hybrid electric vehicles and vehicle-to-grid services," *Environ. Sci. Technol.*, vol. 43, pp. 1199–1204, 2009.

[5] Z. Li, Q. Guo, H. Sun, Y. Wang, and S. Xin, "Emission-concerned wind-EV coordination on the transmission grid side with network constraints: Concept and case study," *IEEE Trans. Smart Grid*, vol. 4, no. 1, pp. 1692–1704, Jan. 2012.

[6] H. Lee and L. Grant, Will Electric Cars Transform the U.S. Market HKS Faculty Research Working Paper Series RWP11-032, John F. Kennedy School of Government, Harvard Univ.. Cambridge, MA, USA, 2011.

[7] Tesla, Features & Specs of Tesla Model S, [Online]. Available: http://www.teslamotors.com/models/features#/performance

[8] Toyota, Prius Plug-In 2014, [Online]. Available: http://www.toyota.com/prius-plug-in/#!/Welcome

[9] Bydauto, e6, [Online]. Available: http://www.bydauto.com.cn/car-show-e6.html

[10] J. C. Gomez and M. M. Morcos, "Impact of EV battery chargers on the power quality of distribution systems," *IEEE Trans. Power Del.*, vol. 22, no. 10, pp. 63–63, Oct. 2002.

[11] G. A. Putrus, P. Suwanapingkarl, D. Johnston, E. C. Bentley, and M. Narayana, "Impact of electric vehicles on power distribution networks," in *Proc. IEEE VPPC*, Chicago, IL, USA, Sep. 2011, pp. 1–6.

[12] Q. Wu, A. H. Nielsen, J. Ostergaard, and S. T. Cha, "Impact study of Electric Vehicle (EV) integration on Medium Voltage (MV) grids," in *Proc. IEEE PES Int. Conf. ISGT Eur.*, Manchester, U.K., Dec. 2011, pp. 1–7.

[13] S. Deilami, A. S. Masoum, P. S. Moses, and M. A. S. Masoum, "Real-time coordination of plug-in electric vehicle charging in smart grids to minimize power losses and improve voltage profile," *IEEE Trans. Smart Grid*, vol. 2, no. 3, pp. 456–467, Sep. 2011.

[14] Y. He, B. Venkatesh, and L. Guan, "Optimal scheduling for charging and discharging of electric vehicles," *IEEE Trans. Smart Grid*, vol. 3, no. 3, pp. 1095–1105, Sep. 2012.

[15] P. Richardson, D. Flynn, and A. Keane, "Optimal charging of electric vehicles in low-voltage distribution systems," *IEEE Trans. Power Syst.*, vol. 27, no. 1, pp. 268–279, Feb. 2012.

[16] L. Gan, U. Topcu, and S. Low, "Optimal decentralized protocol for electric vehicle charging," *IEEE Trans. Power Syst.*, vol. 28, no. 2, pp. 940–951, May 2013.

[17] W. Saad, H. Zhu, H. V. Poor, and T. Basar, "A noncooperative game for double auction-based energy trading between PHEVs and distribution grids," in *Proc. IEEE Int. Conf. SmartGridComm*, Brussels, Belgium, Oct. 2011, pp. 267–272.

[18] H. Ito, "Disturbance and delay robustness of gradient feedback systems based on static noncooperative games with application to PEV charging," in *Proc. 50th IEEE CDC-ECC*, Orlando, FL, USA, Dec. 2011, pp. 325–330.

[19] W. Tushar, W. Saad, H. V. Poor, and D. B. Smith, "Economics of electric vehicle charging: A game theoretic approach," *IEEE Trans. Smart Grid*, vol. 3, no. 4, pp. 1767–1778, Dec. 2012.

[20] C. Wu, H. Mohsenian-Rad, and J. Huang, "Vehicle-to-aggregator interaction game," *IEEE Trans. Smart Grid*, vol. 3, no. 1, pp. 434–442, Mar. 2012.

[21] Z. Ma, D. S. Callaway, and I. A. Hiskens, "Decentralized charging control of large populations of plug-in electric vehicles," *IEEE Trans. Control Syst. Technol.*, vol. 21, no. 1, pp. 67–78, Jan. 2013.

[22] W. Shuo, R. Crosier, and C. Yongbin, "Investigating the power architectures and circuit topologies for megawatt superfast electric vehicle charging stations with enhanced grid support functionality," in *Proc. IEEE Int. Elect. Veh. Conf. (IEVC)*, Greenville, SC, USA, Mar. 2012, pp. 1–8.

[23] M. Etezadi-Amoli, K. Choma, and J. Stefani, "Rapid-charge electric-vehicle stations," *IEEE Trans. Power Del.*, vol. 25, no. 3, pp. 1883–1887, Jul. 2010.

[24] R. Crosier and W. Shuo, "DQ-frame modeling of an active power filter integrated with a grid-connected, multifunctional electric vehicle charging station," *IEEE Trans. Power Electron.*, vol. 28, no. 12, pp. 5702–5716, Dec. 2013.

[25] K. Jiguang, W. Zhenlin, C. Danming, and F. Xu, "Research on electric vehicle charging mode and charging stations construction," (in Chinese) *Power Demand Side Manage.*, vol. 11, no. 5, pp. 64–66, Sep. 2009.

[26] A. S. Masoum, S. Deilami, P. S. Moses, M. A. S. Masoum, and A. Abu-Siada, "Smart load management of plug-in electric vehicles in distribution and residential networks with charging stations for peak shaving and loss minimisation considering voltage regulation," *IET Generat., Transmiss., Distrib.*, vol. 5, pp. 877–888, Jan. 2011.

[27] M. Singh, P. Kumar, and I. Kar, "A multi charging station for electric vehicles and its utilization for load management and the grid support," *IEEE Trans. Smart Grid*, vol. 4, no. 2, pp. 1026–1037, Jun. 2013.

[28] L. Zhipeng, W. Fushuan, and G. Ledwich, "Optimal planning of electric-vehicle charging stations in distribution systems," *IEEE Trans. Power Del.*, vol. 28, no. 1, pp. 102–110, Jan. 2013.

[29] W. Guibin, X. Zhao, W. Fushuan, and P. W. Kit, "Traffic-constrained multiobjective planning of electric-vehicle charging stations," *IEEE Trans. Power Del.*, vol. 28, no. 4, pp. 2363–2372, Oct. 2013.

[30] K. Seongbae, C. Hyung-Chul, L. Jong-Uk, and J. Sung-Kwan, "Probabilistic modeling of electric vehicle charging load for probabilistic load flow," in *Proc. IEEE VPPC*, Seoul, Korea, Oct. 2012, pp. 1010–1013.

[31] T. Ito, Y. Iwafune, and R. Hiwatari, "Evaluation of EV charging load contributing to stabilize PV output with consideration for rapid charge," in *Proc. IEEE ISGT*, Washington, D.C., Jan. 2012, pp. 1–6.

[32] S. Bae and A. Kwasinski, "Spatial and temporal model of electric vehicle charging demand," *IEEE Trans. Smart Grid*, vol. 3, no. 1, pp. 394–403, Mar. 2012.

[33] Baidu Map, [Online]. Available: http://map.baidu.com/

[34] LBS, Cloud BaiduMap API, [Online]. Available: http://developer.baidu.com/map/lbs-cloud.htm

[35] Q. Guo, Y. Wang, H. Sun, Z. Li, and B. Zhang, "Research on architecture of ITS based smart charging guide system," in *Proc. IEEE Power Energy Soc. General Meeting*, Detroit, MI, USA, Jul. 2011, pp. 1–5.

[36] T. Korhonen, T. Väärämäki, V. Riihimäki, R. Salminen, and A. Karila, "Selecting telecommunications technologies for intelligent transport system services in helsinki municipality," *IET Intell. Transport Syst.*, vol. 6, no. 1, pp. 18–28, Mar. 2012.

[37] G. Owojaiye and Y. Sun, "Focal design issues affecting the deployment of wireless sensor networks for intelligent transport systems," *IET Intell. Transport Syst.*, vol. 6, no. 4, pp. 432–432, Dec. 2012.

[38] C. Ming and S. Yuming, "Agent based intelligent transportation management system," in *Proc. IEEE Int. Conf. ITST*, Chengdu, China, Jun. 2006, pp. 190–193.

[39] M. Barth and M. Todd, "Intelligent transportation system architecture for a multi-station shared vehicle system," in *Proc. IEEE Intell. Transp. Syst.*, Dearborn, MI, USA, Oct. 2000, pp. 240–245.

[40] W. Cai and T. Sun, "CTS: The new generation intelligent transportation system," in *Proc. 2rd Int. Conf. IBICA*, Shenzhen, China, Dec. 2011, pp. 137–140.

[41] Z. Fei, "The current situation and development thinking of the intelligent transportation system in China," in *Proc. Int. Conf. MACE*, Wuhan, China, Jun. 2011, pp. 2826–2829.

[42] R. L. Courtney, "A broad view of ITS standards in the US," in *Proc. IEEE Conf. ITSC*, Boston, MA, USA, Nov. 1997, pp. 529–536.

[43] F. Shaojun and L. L. Choi, "Assisted GPS and its impact on navigation in intelligent transportation systems," in *Proc. IEEE Int. Conf. Intell. Transp. Syst.*, Singapore, Nov. 2011, pp. 529–536.

[44] Q. Luo, "Research on intelligent transportation system technologies and applications," in *Proc. PEITS Workshop*, Guangzhou, China, Aug. 2008, pp. 529–531.

[45] Wikipidia on Traffic Message Channel, [Online]. Available: http://en.wikipedia.org/wiki/Traffic_message_channel

[46] VICS, Vehicle Information and Communication System, [Online]. Available: http://www.vics.or.jp/english/vics/index.html

[47] P. Brosch, "A service oriented approach to traffic dependent navigation systems," in *Proc. IEEE Congr. Services—Part I*, Honolulu, HI, USA, Jul. 2008, pp. 269–272.

[48] R. Claes, T. Holvoet, and D. Weyns, "A decentralized approach for anticipatory vehicle routing using delegate multiagent systems," *IEEE Trans. Intell. Transp. Syst.*, vol. 12, no. 2, pp. 364–373, Jan. 2011.

[49] M. Takagi, Y. Iwafune, K. Yamaji, H. Yamamoto, K. Okano, R. Hiwatari, and T. Ikeya, "Economic value of PV energy storage using batteries of battery-switch stations," *IEEE Trans. Sustainable Energy*, vol. 4, no. 1, pp. 164–173, Jan. 2013.

[50] Y. Liu, R. Xu, T. Chen, X. Zhang, R. Wang, and X. Yang, "Investigation on the construction mode of the charging station and battery-swap station," in *Proc. Int. Conf. Elect. Inf. Control Eng.*, Wuhan, China, 2011, pp. 5080–5081.

[51] C. Zheng, L. Nian, X. Xiangning, L. Xinyi, and Z. Jianhua, "Energy exchange model of PV-based battery switch stations based on battery swap service and power distribution," in *Proc. IEEE Veh. Power Propulsion Conf.*, Beijing, China, 2013, pp. 1–6.

[52] J. J. Jamian, M. W. Mustafa, Z. Muda, H. Mokhlis, and M. M. Aman, "Effect of load models on battery-switching station allocation in distribution network," in *Proc. IEEE Int. Conf. Power Energy*, Kota Kinabalu, 2012, pp. 189–193.

[53] M. Yiqun, J. Quanyuan, and C. Yijia, "Battery switch station modeling and its economic evaluation in microgrid," in *Proc. IEEE Power Energy Soc. General Meeting*, San Diego, CA, USA, 2012, pp. 1–7.

[54] Q. Guo, Y. Wang, H. Sun, Z. Li, S. Xin, and B. Zhang, "Factor analysis of the aggregated electric vehicle load based on data mining," *Energies 2012*, vol. 5, no. 6, pp. 2053–2070, 2012.

[55] Z. Darabi and M. Ferdowsi, "Aggregated impact of plug-in hybrid electric vehicles on electricity demand profile," *IEEE Trans. Sustainable Energy*, vol. 2, no. 4, pp. 501–508, Jan. 2011.

[56] A. Rautiainen, S. Repo, P. Jarventausta, A. Mutanen, K. Vuorilehto, and K. Jalkanen, "Statistical charging load modeling of PHEVs in electricity distribution networks using national travel survey data," *IEEE Trans. Smart Grid*, vol. 3, no. 4, pp. 1650–1659, Jan. 2012.

[57] U.S. Department of Transportation, Federal Highway Administration 2009 National Household Travel Survey Home Page, [Online]. Available: http://nhts.ornl.gov

[58] Beijing Municipal Peoples Government, "The Beijing city master plan (2004–2020)," *Beijing City Planning Construction Rev.*, vol. 2, no. 1, pp. 5–51, Mar. 2005.

[59] S. Xin, Q. Guo, H. Sun, Z. Li, B. Zhang, and S. Zhang, "A hybrid simulation method for EVs' operation considering power grid and traffic information," presented at the Proc. IEEE Power and Energy Soc. General Meeting, Vancouver, BC, Canada, Jul. 2013, unpublished.

Qinglai Guo (SM'14) received the B.S. degree from the Department of Electrical Engineering, Tsinghua University, Beijing, China, in 2000 and the Ph.D. degree from Tsinghua University in 2005.

His now an Associate Professor at Tsinghua University. His special fields of interest include EMS advanced applications, especially automatic voltage control and V2G.

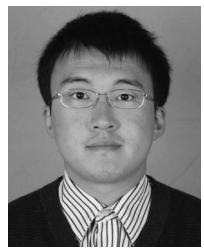

Shujun Xin (S'13) received the Bachelor degree from the Department of Electrical Engineering, Tsinghua University, Beijing, China, in 2012. He is currently pursuing the Master degree in the Department of Electrical Engineering, Tsinghua University.

His research interests include electric vehicles' smart charging and V2G technology.

Hongbin Sun (SM'12) received the double B.S. degrees from Tsinghua University, Beijing, China, in 1992 and the Ph.D. degree from the Department of Electrical Engineering, Tsinghua University in 1997.

He is now Changjiang Chair Professor of Education Ministry of China, Full Professor of electrical engineering in Tsinghua University and Assistant Director of State Key Laboratory of Power Systems in China. From 2007 to 2008, he was a Visiting Professor with School of Electrical Engineering and Computer Science, Washington State University, Pullman, WA, USA. In the last 15 years, he has developed a commercial system-wide automatic voltage control systems which has been applied to more than 20 large-scale power grids in China. He published more than 200 academic papers. He held more than 20 patents in China.

Prof. Sun is an IET Fellow, members of IEEE PES CAMS Cascading Failure Task Force and CIGRE C2.13 Task Force on Voltage/Var support in System Operations. He won the China National Technology Innovation Award for his contribution on successful development and applications of New Generation of EMS for Power Systems in 2008, the National Distinguished Teacher Award in China for his contribution on power engineering education in 2009, and the National Science Fund for Distinguished Young Scholars of China for his contribution on power system operation and control in 2010.

Zhengshuo Li (S'12) received the Bachelor degree from the Department of Electrical Engineering, Tsinghua University, Beijing, China, in 2011. He is currently pursuing the Ph.D. degree in the Department of Electrical Engineering, Tsinghua University.

His research interests include electric vehicle smart charging and V2G technology.

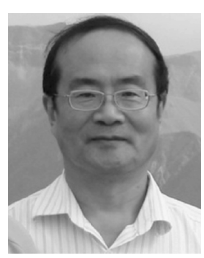

Boming Zhang (SM'95–F'10) received the Ph.D. degree in electrical engineering from Tsinghua University, Beijing, China, in 1985.

Since 1985, he has been with the Electrical Engineering Department, Tsinghua University, for teaching and research and promoted to a Professor in 1993. His interest is in power system analysis and control, especially in the EMS advanced applications in the Electric Power Control Center (EPCC). He has published more than 300 academic papers and implemented more than 60 EMS/DTS systems in China.

Prof. . Zhang is now a steering member of CIGRE China State Committee and of the International Workshop of EPCC.